

Computer-generated hologram using binary phase with an aperture

WEN CHEN^{1,2,*}

¹The Hong Kong Polytechnic University Shenzhen Research Institute, Shenzhen 518057, China

²Department of Electronic and Information Engineering, The Hong Kong Polytechnic University, Hong Kong, China

*Corresponding author: owen.chen@polyu.edu.hk

Received XX Month XXXX; revised XX Month, XXXX; accepted XX Month XXXX; posted XX Month XXXX (Doc. ID XXXXX); published XX Month XXXX

Computer-generated hologram (CGH) has attracted more and more attention in some application fields, such as 3D display, optical security and beam shaping. In this paper, a strategy is presented for optical information verification based on CGH using binary phase (1-bit) with an aperture. The input is encoded into the cascaded phase-only masks based on CGH via iterative phase retrieval, and one extracted phase mask is binarized in which one part is selected according to an aperture and further embedded into a random binary-phase host mask. It is numerically illustrated that the reconstructed image can be effectively verified, when system parameters, such as aperture and phase-only masks, are correctly applied. It is demonstrated that the proposed method can provide a promising strategy for CGH-based optical verification. © 2017 Optical Society of America

OCIS codes: (200.4740) Optical processing; (200.4560) Optical data processing.

<http://dx.doi.org/10.1364/AO.99.099999>

1. INTRODUCTION

Since computer-generated hologram (CGH) [1] was proposed, it has been becoming one of the most popular and important methods in some application areas, such as display and beam shaping. There are several approaches for computing CGH [2–7], such as iteration [2], fast generation using warping [3], ray-tracing [4], angular-spectrum layer-oriented method [5] and down sampling [7]. For instance, Gerchberg-Saxton algorithm [8] and its derivatives [9] are commonly applied to generate phase CGH. In the ray-tracing method, fringe pattern for each object point is individually calculated by diffraction and interference, and in the look-up table method each elemental fringe pattern corresponding to a point source is pre-calculated and stored for improving the computational speed.

Since double random phase encoding (DRPE) [10] was proposed, many optical security structures [11–29] have been developed. The CGH via iterative phase retrieval has also been applied for optical encoding and verification. The CGH via phase retrieval [21–29] is considered as one of the most important technologies due to its remarkable characteristics, such as convenient implementation by optics. It is demonstrated [21–29] that the input can be iteratively encoded. Phase-only masks extracted in phase-retrieval-based encoding systems [21–29] can be considered as CGH in essence, and phase retrieval approach is usually developed by using Gerchberg-Saxton (GS) algorithm [8] via an iterative operation. For instance, Wang et al. [21] encoded

the input data into phase-only masks, and Hwang et al. [24] applied the GS algorithm with a phase modulation method for optical multiple-image encoding. In addition, different transfer domains [21–30], such as gyrator transform [26], have been flexibly integrated into the CGH system for optical encoding.

The CGH system via iterative phase retrieval has also been found to be a promising and effective method for optical information verification [31]. For instance, the extracted phase mask can be compressed [31], and only some sparse pixels in the extracted phase mask are available to the receivers. Hence, nonlinear correlation algorithm [31–45] can be further applied to verify the decoded images without information disclosure by connecting to a remote database. It is demonstrated [31,38] that it is possible to generate a new layer to enhance CGH-based system security.

However, phase distributions that are larger than 2-bit are usually applied in the CGH-based optical encryption and verification infrastructures. By using the lower-bit phase-only maps, it is possible to apply the cheaper optical components in the CGH-based optical information security systems.

In this paper, inspired by the works in Refs. [22,27,31,45], a strategy is presented for optical information verification based on CGH using binary phase (1-bit) with an aperture. The input is encoded into the cascaded phase-only masks based on CGH via iterative phase retrieval, and one extracted mask is binarized in which one part is selected according to an aperture and further embedded into a random binary-phase host mask. It will be demonstrated that the reconstructed images can be effectively

verified based on CGH system, and a promising strategy can be established for optical information verification.

2. PRINCIPLES

Figure 1 shows a schematic arrangement for the proposed method based on CGH. The input is iteratively encoded into the cascaded phase masks, and a digital approach is applied for the encoding. The main objective of encoding process is to obtain the approximated phase masks, when the related constraints [22,27,28,31], such as input image and setup parameters, are available.

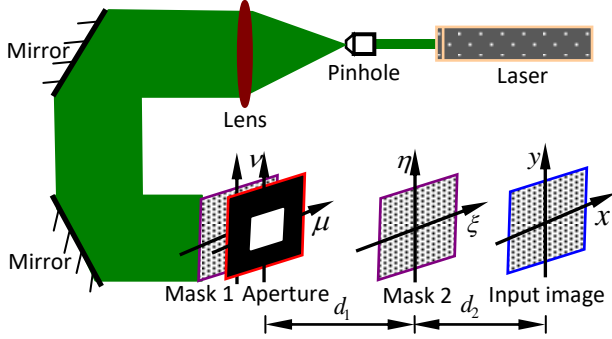


Fig. 1. A schematic for the proposed method using phase-only CGH. An aperture is used and can be placed behind mask 1, and it is straightforward to place it just before mask 1. Mask 1 denotes $M_1(\mu, \nu)$, and mask 2 denotes $M_2(\xi, \eta)$. Since strategy with binarization and aperture is applied, the proposed method based on phase-only CGH is more suitable for encoding and verifying binary input images. In practice, the aperture may also be directly generated by using spatial light modulator.

To encode the input, M1 and M2 should be initialized, i.e., randomly in a range of $[0, 2\pi]$. Let $M_1^{(n)}(\mu, \nu)$ and $M_2^{(n)}(\xi, \eta)$ ($n=1, 2, 3, \dots, N$) respectively denote M1 and M2. Wavefront $O^{(n)}(x, y)$ in input image plane is described by

$$O^{(n)}(x, y) = \text{FrT}_{\lambda, d_2} \left(\left\{ \text{FrT}_{\lambda, d_1} \left[M_1^{(n)}(\mu, \nu) \right] \right\} M_2^{(n)}(\xi, \eta) \right), \quad (1)$$

where λ denotes the wavelength, d_1 and d_2 denote axial distances, and FrT denotes wave propagation in free space [30]. (μ, ν) , (ξ, η) and (x, y) respectively denote coordinates of M1 plane, M2 plane and input image plane.

Subsequently, constraint [22,27,28,31,38] is applied to generate an updated wavefront $\hat{O}^{(n)}(x, y)$.

$$\hat{O}^{(n)}(x, y) = \sqrt{I(x, y)} O^{(n)}(x, y) / |O^{(n)}(x, y)|, \quad (2)$$

where $I(x, y)$ denotes the input image, and $||$ denotes a modulus operation. Hence, M2 can be updated by [27,28,31]

$$\hat{M}_2^{(n)}(\xi, \eta) = \left(\frac{\text{FrT}_{\lambda, -d_2} \left[\hat{O}^{(n)}(x, y) \right]}{\text{FrT}_{\lambda, d_1} \left[M_1^{(n)}(\mu, \nu) \right]} \right) \left/ \left| \frac{\text{FrT}_{\lambda, -d_2} \left[\hat{O}^{(n)}(x, y) \right]}{\text{FrT}_{\lambda, d_1} \left[M_1^{(n)}(\mu, \nu) \right]} \right| \right., \quad (3)$$

where $\text{FrT}_{\lambda, -d_2}$ denotes wave back-propagation in free space [30], and $\hat{M}_2^{(n)}(\xi, \eta)$ denotes an updated phase mask M2.

Subsequently, an updated phase mask M1 $\hat{M}_1^{(n)}(\mu, \nu)$ can be obtained by [22,31]

$$\hat{M}_1^{(n)}(\mu, \nu) = \frac{\text{FrT}_{\lambda, -d_1} \left(\left\{ \text{FrT}_{\lambda, -d_2} \left[\hat{O}^{(n)}(x, y) \right] \right\} \left[\hat{M}_2^{(n)}(\xi, \eta) \right]^* \right)}{\left| \text{FrT}_{\lambda, -d_1} \left(\left\{ \text{FrT}_{\lambda, -d_2} \left[\hat{O}^{(n)}(x, y) \right] \right\} \left[\hat{M}_2^{(n)}(\xi, \eta) \right]^* \right) \right|}, \quad (4)$$

where $\text{FrT}_{\lambda, -d_1}$ denotes wave back-propagation in free space [30], and asterisk denotes complex conjugate. The difference between estimated and desired outputs [22,27,28,31] is evaluated to determine whether the iterative process can be stopped. Here, correlation coefficient (CC) is calculated to evaluate the difference. When the calculated CC value is big enough (i.e., bigger than a threshold of 0.999), $\hat{M}_1^{(n)}(\mu, \nu)$ and $\hat{M}_2^{(n)}(\xi, \eta)$ can be considered as the desired phase-only CGHs, i.e., $M_1(\mu, \nu)$ and $M_2(\xi, \eta)$. Otherwise, the updated masks obtained in Eqs. (3) and (4) are further used (i.e., iterative number $n=n+1$).

Here, to implement image verification without disclosure of the input image, the extracted mask $M_1(\mu, \nu)$ is further binarized [45] as $M_{1b}(\mu, \nu)$ which is described by

$$\text{angle}[M_{1b}(\mu, \nu)] = \begin{cases} 1 & \text{if } \text{angle}[M_1(\mu, \nu)] \geq \text{Ave}\{\text{angle}[M_1(\mu, \nu)]\} \\ 0 & \text{if } \text{angle}[M_1(\mu, \nu)] < \text{Ave}\{\text{angle}[M_1(\mu, \nu)]\} \end{cases}, \quad (5)$$

where angle denotes phase component, and Ave denotes the average value. Subsequently, only one part of the binarized phase mask $M_{1b}(\mu, \nu)$ is selected according to a designed aperture as follows:

$$\hat{M}_{1b}(\mu, \nu) = \begin{cases} M_{1b}(\mu, \nu) & \text{if } (\mu, \nu) \in A(\mu, \nu) \\ 0 & \text{if } (\mu, \nu) \notin A(\mu, \nu) \end{cases}, \quad (6)$$

where $A(\mu, \nu)$ denotes the designed aperture, and $\hat{M}_{1b}(\mu, \nu)$ denotes the selected part of binarized mask M1 [i.e., from $M_{1b}(\mu, \nu)$]. Finally, the pixels (i.e., within the aperture) in $\hat{M}_{1b}(\mu, \nu)$ directly replace the corresponding pixels in a pre-set random-binary-phase host mask to generate the final binary phase mask M1, i.e., $M_{1b}(\mu, \nu)$. Alternatively, $M_2(\xi, \eta)$ can also be binarized.

During optical recovery, $M_{1b}(\mu, \nu)$ and $M_2(\xi, \eta)$ are available to the authorized receiver, and the aperture should be correctly applied. The recovery process can be described by

$$\hat{O}(x, y) = \left| \text{FrT}_{\lambda, d_2} \left(\left\{ \text{FrT}_{\lambda, d_1} \left[M_{1b}(\mu, \nu) A(\mu, \nu) \right] \right\} M_2(\xi, \eta) \right) \right|^2, \quad (7)$$

where $\hat{O}(x, y)$ denotes a recovered image. As seen in Fig. 1, the aperture is placed just behind M1 during image recovery. Since only a small part of binary-phase mask $M_{1b}(\mu, \nu)$ contains useful information, the recovered image is noisy even by using correct parameters. Due to the application of binarization operation and an aperture, the recovered image cannot visually render information about the input image. However, useful information related to the input image is still available in the recovered image.

Instead of direct observation of the input, nonlinear correlation algorithm [22,27,31–45] is applied to verify the recovered image.

$$NC(x,y) = \left| \text{IFT} \left(\left\{ \text{FT} [I(x,y)] \right\} \left\{ \text{FT} [\hat{O}(x,y)] \right\}^{*w-1} \right) \right| \times \left\{ \text{FT} [I(x,y)] \right\} \left\{ \text{FT} [\hat{O}(x,y)] \right\}^* \right|^2, \quad (8)$$

where $NC(x,y)$ is the verification distribution, FT denotes Fourier transform, and IFT denotes inverse Fourier transform. Other correlation algorithms [46–48] can also be applicable. In practice, original input image $I(x,y)$ can be placed in an independent database [49], and the receiver can use an interface to conduct information verification without directly viewing original input image. A flow chart in Fig. 2 shows the whole process aforementioned.

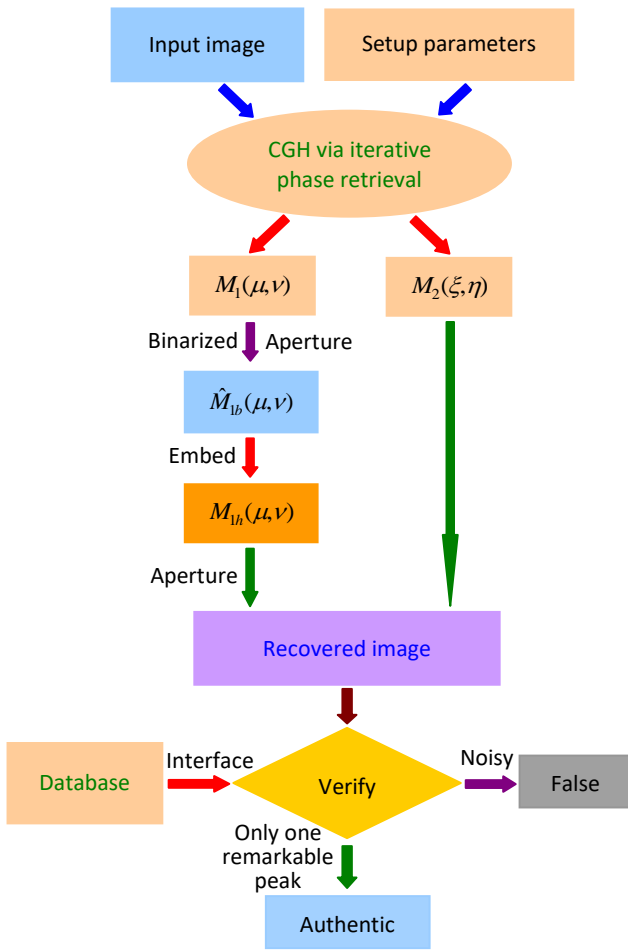


Fig. 2. A flow chart to illustrate mask generation, image recovery and verification process.

3. Results and discussion

The setup in Fig. 1 is numerically conducted to show the validity. The plane wave is generated to illuminate phase mask, and laser wavelength is 600.0 nm. d_1 and d_2 are 17.0 cm and 12.0 cm, respectively. The extracted phase masks can be embedded into phase plate or spatial light modulators (4.65 μm and

512×512 pixels) during the recovery. A digital approach should be applied for the generation of $M_{1h}(\mu,\nu)$ and $M_2(\xi,\eta)$, and digital and optical approaches can be flexibly selected for the recovery and optical verification.

Figure 3(a) shows an input image (pixels of 512×512), and Fig. 3(b) shows a relationship to illustrate an iterative process when CGH via iterative phase retrieval is applied. It is seen in Fig. 3(b) that a rapid convergence rate, i.e., only 10 iterations, is achieved. Figures 3(c) and 3(d) show the extracted masks $M_1(\mu,\nu)$ and $M_2(\xi,\eta)$, respectively. In the proposed method, $M_1(\mu,\nu)$ is further binarized, and only a small part of its binary version is selected according to a designed aperture. Figure 3(e) shows an aperture, and Fig. 3(f) shows the final binary-phase host mask $M_{1h}(\mu,\nu)$. As seen in Fig. 3(f), it is difficult to identify which part in the binary-phase mask $M_{1h}(\mu,\nu)$ is useful for subsequent recovery. One small region in Fig. 3(f) has been enlarged to clearly illustrate the binarization. In practice, the finally generated masks $M_{1h}(\mu,\nu)$ and $M_2(\xi,\eta)$ can be transmitted to the receiver. When all parameters are correctly applied, a recovered image is shown in Fig. 4(a). CC value for Fig. 4(a) is 0.079. It can be seen in Fig. 4(a) that only noisy distribution is obtained due to the proposed strategy with binarization and aperture. This recovered image is further verified [22,27,31–45,50–54], and a verification distribution corresponding to Fig. 4(a) is shown in Fig. 4(b). Only one remarkable peak is generated over noisy background, and it means that the recovered image is authentic and the receiver has correct keys. In practice, other matching parameters can also be pre-set and used for the judgment.

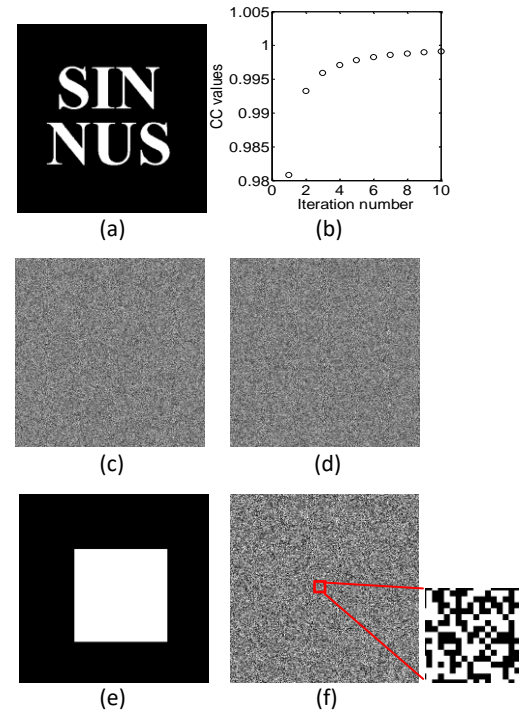


Fig. 3. (a) An input image (pixels of 512×512), (b) a relationship to illustrate the iterative encryption process when CGH via iterative phase retrieval is applied, (c) $M_1(\mu,\nu)$ and (d) $M_2(\xi,\eta)$, (e) an aperture, and (f) the final binary-phase host mask $M_{1h}(\mu,\nu)$. An inset is given to clearly illustrate the operation.

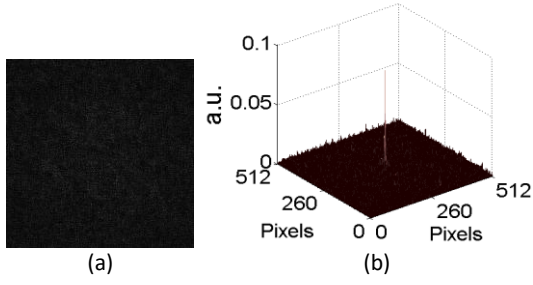


Fig. 4. (a) A recovered image generated when a receiver applies correct parameters, and (b) verification distribution corresponding to (a).

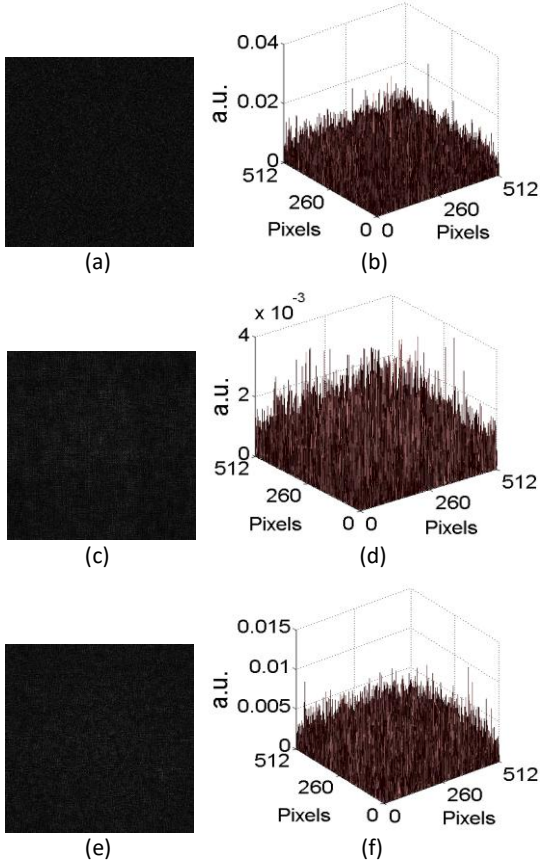


Fig. 5. (a) A recovered image generated when binary-phase host mask $M_{in}(\mu, \nu)$ is used without the aperture, (b) the verification distribution corresponding to (a); (c) a recovered image obtained when only the aperture is wrongly applied for the reconstruction, (d) the verification distribution corresponding to (c); (e) a recovered image obtained when only phase-only mask M2 [i.e., $M_2(\xi, \eta)$] is incorrectly applied for the recovery, (f) the verification distribution corresponding to (e).

Performance of system parameters is analyzed. Figure 5(a) shows a recovered image, when the random binary-phase host mask $M_{in}(\mu, \nu)$ is used without the aperture. The CC value for Fig. 5(a) is 0.020. Figure 5(b) shows the verification distribution generated by nonlinear correlation algorithm corresponding to Fig. 5(a). It is seen in Fig. 5(b) that only noisy distribution without remarkable peaks is obtained. Figure 5(c) shows a recovered image, when only the aperture is wrongly applied for the

reconstruction. The CC value for Fig. 5(c) is 0.031. Figure 5(d) shows the verification distribution generated by nonlinear correlation algorithm corresponding to Fig. 5(c). Figure 5(e) shows a recovered image, when only the phase-only mask M2 [i.e., $M_2(\xi, \eta)$] is incorrectly applied for the recovery. The CC value for Fig. 5(e) is 0.010. Figure 5(f) shows the verification distribution generated by nonlinear correlation algorithm corresponding to Fig. 5(e). It has been illustrated in Figs. 5(b), 5(d) and 5(f) that phase masks and the aperture are important parameters for optical information verification.

System robustness, i.e., against noise contamination, is further tested. Figure 6(a) shows a recovered image, when the finally generated masks $M_{in}(\mu, \nu)$ and $M_2(\xi, \eta)$ [respectively in Figs. 3(f) and 3(d)] are contaminated by additive white noise [31] (zero mean noise with 0.10 variance). Correct parameters, such as setup parameters and aperture, have been applied for the recovery in Fig. 6(a). CC value for Fig. 6(a) is 0.068. Figure 6(b) shows a verification distribution corresponding to Fig. 6(a). It is illustrated that only one remarkable peak can still be generated. Useful information on recovered image is still sufficient to be verified. The proposed method shows high robustness against noise contamination.

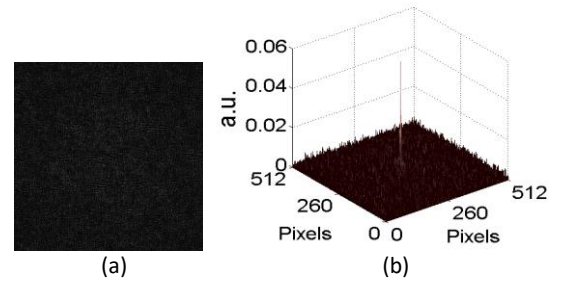


Fig. 6. (a) A recovered image obtained when $M_{in}(\mu, \nu)$ and $M_2(\xi, \eta)$ are contaminated, and (b) verification distribution corresponding to (a).

The discrimination capability is also tested, when another input image [see Fig. 7(a)] is processed using the same parameters as those used for Figs. 3 and 4. Figure 7(b) shows a relationship for the iterations obtained during the encoding, when CGH via iterative phase retrieval is applied. Figure 7(c) shows a recovered image, when correct parameters are employed during the reconstruction. Due to the developed strategy with binarization and aperture, it can be seen that information related to the second input image cannot be clearly observed. Figure 7(d) shows the corresponding nonlinear correlation distribution between that in Fig. 7(c) and the original input image [i.e., Fig. 3(a)]. As seen in Fig. 7(d), only noisy background is generated, and the proposed optical verification system possesses high discrimination capability. Some other tests using different input images have also been conducted, and similar results are always generated.

High flexibility to design the aperture can be achieved in the proposed method. Figures 8(a) and 8(b) show the apertures located at the positions which are different from that in Fig. 3(e). Figures 8(c) and 8(e) show the recovery and verification results, when the aperture in Fig. 8(a) is applied and all parameters are correctly used. Figures 8(d) and 8(f) show the recovery and verification results, when the aperture in Fig. 8(b) is applied and all parameters are correctly used. The CC values for Figs. 8(c) and

8(d) are 0.072 and 0.075, respectively. It is illustrated in Figs. 8(c)–8(f) that aperture positions can be flexibly designed. In practice, aperture size and shape can also be adjusted.

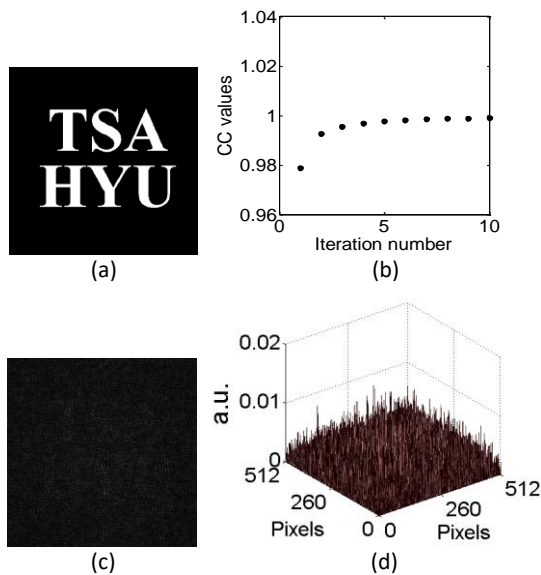


Fig. 7. (a) Another input, (b) a relationship to illustrate the iterative encryption process when CGH via iterative phase retrieval is applied, (c) a recovered image obtained when correct parameters are used during the reconstruction, and (d) nonlinear correlation distribution generated between that in (c) and the original input image in Fig. 3(a).

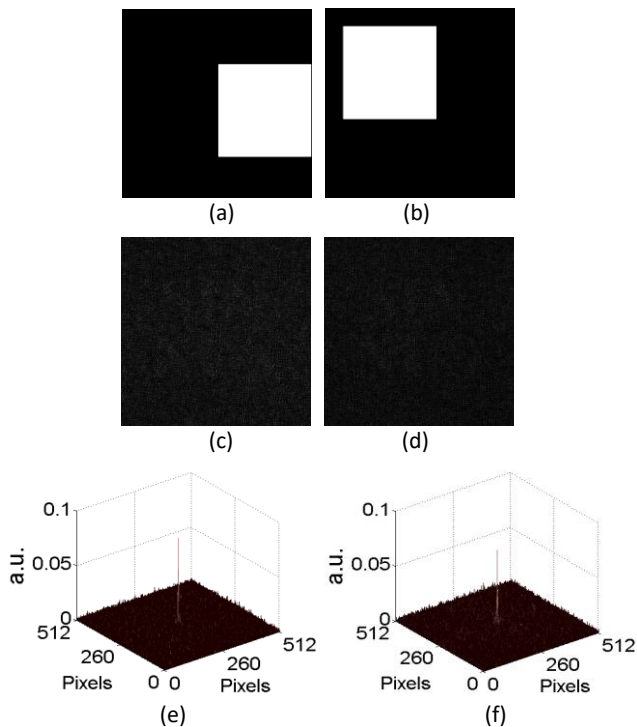


Fig. 8. (a) and (b) The apertures located at the different positions, (c) and (e) recovery and verification results obtained when the aperture in (a) is applied and all parameters are correctly used, (d) and (f) recovery and verification results obtained when the aperture in (b) is applied and all parameters are correctly used.

The advantages and the difference compared to conventional methods are further described and discussed: (1) Binary phase is applied based on CGH via phase retrieval for optical information verification, hence the cost for at least one device (such as phase-only spatial light modulator) can be reduced since 1-bit optical component is requested. (2) Different from previous works [22,27,28,31,38], the proposed optical system based on CGH uses binary phase rather than sparse phase (i.e., usually larger than 2 bit). In addition, a simple method with an aperture has been introduced to hide the binary-phase information. The proposed method can provide a strategy for effectively conducting information verification based on CGH via iterative phase retrieval. (3) Different from those in Refs. [44,45,53], binarization operation with an aperture has been successfully applied in the CGH system rather than conventional DRPE infrastructure, hence a novel implementation strategy has been established for optical verification. The method presented here can be applied to enrich variety of optical information verification systems [44,45,49,53]. (4) High flexibility is achieved in the proposed method. The aperture size, shape and position can be flexibly modified, and aperture array can also be applied in practice. A different aperture can also be placed just behind M2, and M2 may be binarized for encoding and verifying different binary input images. In addition, the input image may be sparsified before the encoding [22,45]. Different cascaded phase structures can also be employed to enhance system complexity to the attackers.

4. Conclusions

A method has been presented for optical information verification based on CGH using binary phase (1-bit) with an aperture. The input is encoded into noisy phase masks by using CGH via iterative phase retrieval, and one extracted phase mask is binarized in which one part is selected according to an aperture and further embedded into a random binary-phase host mask. The numerical results demonstrate that when the extracted phase masks and the aperture are correctly applied, the recovered image can be effectively verified. It has also been illustrated that the proposed optical verification method possesses high robustness and flexibility. The proposed method is suitable for verifying binary input images.

Funding. National Natural Science Foundation of China (NSFC) (61605165); Hong Kong Research Grants Council Early Career Scheme (25201416); Shenzhen Science and Technology Innovation Commission through Basic Research Program (JCY20160531184426473); The Hong Kong Polytechnic University (1-ZE5F, 4-BCDY and 4-ZZHM).

References

1. A. W. Lohmann and D. P. Paris, "Binary Fraunhofer holograms, generated by computer," *Appl. Opt.* **6**, 1739–1748 (1967).
2. M. Makowski, M. Sypek, and A. Kolodziejczyk, "Colorful reconstructions from a thin multi-plane phase hologram," *Opt. Express* **16**, 11618–11623 (2008).
3. P. W. M. Tsang and T. C. Poon, "Fast generation of digital holograms based on warping of the wavefront recording plane," *Opt. Express* **23**, 7667–7673 (2015).

4. C. J. Kuo and M. H. Tsai, *Three-Dimensional Holographic Imaging*, John Wiley & Sons, 2002.
5. Y. Zhao, L. C. Cao, H. Zhang, D. Kong, and G. F. Jin, "Accurate calculation of computer-generated holograms using angular-spectrum layer-oriented method," *Opt. Express* **23**, 25440–25449 (2015).
6. J. Wang and Y. L. Sheng, "Computer-generated very large space-bandwidth product binary hologram for laser projector," *IEEE Trans. Ind. Informat.* **12**, 179–186 (2016).
7. P. W. M. Tsang, Y. T. Chow, and T. C. Poon, "Generation of phase-only Fresnel hologram based on down-sampling," *Opt. Express* **22**, 25208–25214 (2014).
8. R. W. Gerchberg and W. O. Saxton, "A practical algorithm for the determination of phase from image and diffraction plane pictures," *Optik (Stuttgart)* **35**, 237–246 (1972).
9. J. R. Fienup, "Phase retrieval algorithms: a comparison," *Appl. Opt.* **21**, 2758–2769 (1982).
10. P. Refregier and B. Javidi, "Optical image encryption based on input plane and Fourier plane random encoding," *Opt. Lett.* **20**, 767–769 (1995).
11. N. K. Nishchal, J. Joseph, and K. Singh, "Fully phase encryption using fractional Fourier transform," *Opt. Eng.* **42**, 1583–1588 (2003).
12. Y. Zhang and B. Wang, "Optical image encryption based on interference," *Opt. Lett.* **33**, 2443–2445 (2008).
13. B. Javidi, A. Sergent, and E. Ahouzi, "Performance of double phase encoding encryption technique using binarized encrypted images," *Opt. Eng.* **37**, 565–569 (1998).
14. W. Chen, X. Chen, and C. J. R. Sheppard, "Optical image encryption based on diffractive imaging," *Opt. Lett.* **35**, 3817–3819 (2010).
15. W. Qin and X. Peng, "Asymmetric cryptosystem based on phase-truncated Fourier transforms," *Opt. Lett.* **35**, 118–120 (2010).
16. W. Chen and X. Chen, "Optical cryptography topology based on a three-dimensional particle-like distribution and diffractive imaging," *Opt. Express* **19**, 9008–9019 (2011).
17. Z. Liu, Q. Guo, L. Xu, M. A. Ahmad, and S. Liu, "Double image encryption by using iterative random binary encoding in gyrator domains," *Opt. Express* **18**, 12033–12043 (2010).
18. X. Wang, D. Zhao, F. Jing, and X. Wei, "Information synthesis (complex amplitude addition and subtraction) and encryption with digital holography and virtual optics," *Opt. Express* **14**, 1476–1486 (2006).
19. Y. Shi, T. Li, Y. Wang, Q. Gao, S. Zhang, and H. Li, "Optical image encryption via ptychography," *Opt. Lett.* **38**, 1425–1427 (2013).
20. A. Alfalou and C. Brosseau, "Optical image compression and encryption methods," *Adv. Opt. Photon.* **1**, 589–636 (2009).
21. R. K. Wang, I. A. Watson, and C. Chatwin, "Random phase encoding for optical security," *Opt. Eng.* **35**, 2464–2469 (1996).
22. W. Chen, "Computer-generated hologram authentication via optical correlation," 2016 IEEE 14th International Conference on Industrial Informatics (INDIN), Poitiers, 2016, pp. 536–540. doi: 10.1109/INDIN.2016.7819220.
23. H. T. Chang, W. C. Lu, and C. J. Kuo, "Multiple-phase retrieval for optical security systems by use of random-phase encoding," *Appl. Opt.* **41**, 4825–4834 (2002).
24. H. E. Hwang, H. T. Chang, and W. N. Lie, "Multiple-image encryption and multiplexing using a modified Gerchberg-Saxton algorithm and phase modulation in Fresnel-transform domain," *Opt. Lett.* **34**, 3917–3919 (2009).
25. G. Situ and J. Zhang, "A lensless optical security system based on computer-generated phase only masks," *Opt. Commun.* **232**, 115–122 (2004).
26. Z. Liu, L. Xu, C. Lin, and S. Liu, "Image encryption by encoding with a nonuniform optical beam in gyrator transform domains," *Appl. Opt.* **49**, 5632–5637 (2010).
27. W. Chen, X. Wang, and X. Chen, "Security-enhanced phase encryption assisted by nonlinear optical correlation via sparse phase," *J. Opt.* **17**, 035702 (2015).
28. W. Chen, B. Javidi, and X. Chen, "Advances in optical security systems," *Adv. Opt. Photon.* **6**, 120–155 (2014).
29. Y. L. Xiao, X. Zhou, S. Yuan, Q. Liu, and Y. C. Li, "Multiple-image optical encryption: an improved encoding approach," *Appl. Opt.* **48**, 2686–2692 (2009).
30. J. W. Goodman, *Introduction to Fourier Optics* 2nd ed. New York, McGraw-Hill, 1996.
31. W. Chen, X. Chen, A. Stern, and B. Javidi, "Phase-modulated optical system with sparse representation for information encoding and authentication," *IEEE Photon. J.* **5**, 6900113 (2013).
32. B. Javidi, "Nonlinear joint power spectrum based optical correlation," *Appl. Opt.* **28**, 2358–2367 (1989).
33. E. Pérez-Cabré, M. Cho, and B. Javidi, "Information authentication using photon-counting double-random-phase encrypted images," *Opt. Lett.* **36**, 22–24 (2011).
34. D. Maluenda, A. Carnicer, R. Martínez-Herrero, I. Juvells, and B. Javidi, "Optical encryption using photon-counting polarimetric imaging," *Opt. Express* **23**, 655–666 (2015).
35. E. Pérez-Cabré, H. C. Abril, M. S. Millan, and B. Javidi, "Photon-counting double-random-phase encoding for secure image verification and retrieval," *J. Opt.* **14**, 094001 (2012).
36. W. Chen and X. Chen, "Ghost imaging for three-dimensional optical security," *Appl. Phys. Lett.* **103**, 221106 (2013).
37. W. Chen and X. Chen, "Object authentication in computational ghost imaging with the realizations less than 5% of Nyquist limit," *Opt. Lett.* **38**, 546–548 (2013).
38. W. Chen and X. Chen, "Optical multiple-image authentication based on modified Gerchberg-Saxton algorithm with random sampling," *Opt. Commun.* **318**, 128–132 (2014).
39. J. X. Chen, Z. L. Zhu, C. Fu, H. Yu, and L. B. Zhang, "Gyrator transform based double random phase encoding with sparse representation for information authentication," *Opt. Laser Technol.* **70**, 50–58 (2015).
40. X. Wang, W. Chen, and X. Chen, "Optical information authentication using compressed double-random-phase-encoded images and quick-response codes," *Opt. Express* **23**, 6239–6253 (2015).
41. W. Chen and X. Chen, "Marked ghost imaging," *Appl. Phys. Lett.* **104**, 251109 (2014).
42. X. Wang, W. Chen, and X. Chen, "Optical encryption and authentication based on phase retrieval and sparsity constraints," *IEEE Photon. J.* **7**, 7800310 (2015).
43. W. Chen, "Multiple-wavelength double random phase encoding with CCD-plane sparse-phase multiplexing for optical information verification," *Appl. Opt.* **54**, 10711–10716 (2015).
44. W. Chen, "Single-shot imaging without reference wave using binary intensity pattern for optically-secured-based correlation," *IEEE Photon. J.* **8**, 6900209 (2016).
45. W. Chen and X. Chen, "Digital holography-secured scheme using only binary phase or amplitude as ciphertext," *Appl. Opt.* **55**, 6740–6746 (2016).
46. S. Jin and S. Y. Lee, "Joint transform correlator with fractional Fourier transform," *Opt. Commun.* **207**, 161–168 (2002).
47. F. Sadjadi and B. Javidi, *Physics of the Automatic Target Recognition*, Springer, Berlin, 2007.
48. S. K. Rajput, D. Kumar, and N. K. Nishchal, "Photon counting imaging and phase mask multiplexing for multiple images authentication and digital hologram security," *Appl. Opt.* **54**, 1657–1666 (2015).
49. W. Chen and X. Chen, "Grayscale object authentication based on ghost imaging using binary signals," *EPL* **110**, 44002 (2015).
50. X. Wang, W. Chen, S. Mei, and X. Chen, "Optically secured information retrieval using two authenticated phase-only masks," *Sci. Rep.* **5**, 15668 (2015).
51. D. Fan, X. F. Meng, Y. Wang, X. Yang, X. Pan, X. Peng, W. Q. He, G. Dong, and H. Chen, "Multiple-image authentication with a cascaded multilevel architecture based on amplitude field random sampling and phase information multiplexing," *Appl. Opt.* **54**, 3204–3215 (2015).
52. W. Chen, G. Situ, and X. Chen, "High-flexibility optical encryption via aperture movement," *Opt. Express* **21**, 24680–24691 (2013).
53. W. Chen and X. Chen, "Double random phase encoding using phase reservation and compression," *J. Opt.* **16**, 025402 (2014).

54. W. Chen, "Ghost identification based on single-pixel imaging in big data environment," *Opt. Express* **25**, 16509–16516 (2017).